TLR1/2 ligand enhances antitumor efficacy of CTLA-4 blockade by increasing intratumoral Treg depletion

Naveen Sharma[a,1], Jean Vacher[b], and James P. Allison[a,c,1]

[a]Department of Immunology, The University of Texas MD Anderson Cancer Center, Houston, TX 77030; [b]Institut de Recherches Cliniques de Montréal, Department of Medicine, University of Montreal, Montreal, QC H2W 1R7, Canada; and [c]Parker Institute for Cancer Immunotherapy, The University of Texas MD Anderson Cancer Center, Houston, TX 77030

Edited by Tak W. Mak, The Campbell Family Institute for Breast Cancer Research at Princess Margaret Cancer Centre, University Health Network, Toronto, ON, Canada, and approved April 16, 2019 (received for review November 5, 2018)

Immune checkpoint inhibitors such as anti–CTLA-4 antibody are widely accepted therapeutic options for many cancers, but there is still a considerable gap in achieving their full potential. We explored the potential of activating the innate and adaptive immune pathways together to improve tumor reduction and survival outcomes. We treated a mouse model of melanoma with intratumoral injections of Toll-like receptor 1/2 (TLR1/2) ligand Pam3CSK4 plus i.p. injections of anti–CTLA-4 antibody. This combination treatment enhanced antitumor immune responses both qualitatively and quantitatively over anti–CTLA-4 alone, and its efficacy depended on CD4 T cells, CD8 T cells, Fcγ receptor IV, and macrophages. Interestingly, our results suggest a unique mechanism by which TLR1/2 ligand increased Fcγ receptor IV expression on macrophages, leading to antibody-dependent macrophage-mediated depletion of regulatory T cells in the tumor microenvironment and increasing efficacy of anti–CTLA-4 antibody in the combination treatment. This mechanism could be harnessed to modulate the clinical outcome of anti–CTLA-4 antibodies and possibly other antibody-based immunotherapies.

tumor immunotherapy | CTLA-4 | anti–CTLA-4 antibody | TLR1/2 ligand | melanoma

Costimulatory/coinhibitory receptors on T cells, which are part of the adaptive immune system, are promising targets in cancer immunotherapy. One successful strategy for therapeutically targeting the inhibitory receptors is to prevent their interaction with their ligands by administering blocking antibodies such as ipilimumab, a checkpoint inhibitor that targets the inhibitory receptor cytotoxic T lymphocyte-associated antigen 4 (1, 2). Anti–CTLA-4 antibodies mediate antitumor activity by blocking inhibitory signals on effector T cells (Teffs), enhancing Teff proliferation, and altering the Teff/regulatory T cell (Treg) ratio (3, 4). We previously found that anti–CTLA-4 antibody depletes tumor-infiltrating Tregs in the mouse B16 melanoma model, which expresses granulocyte macrophage colony-stimulating factor (GM-CSF), representing another mechanism by which anti–CTLA-4 antibody has antitumor activity (5). Fcγ receptor IV on macrophages has been implicated in the anti–CTLA-4 antibody-mediated depletion of Tregs in this model.

Although checkpoint inhibitors such as anti–CTLA-4 antibody have been effective in treating some cancers, many patients either do not respond or develop resistance, and complete cures with single immunotherapy agents occur in a minority of patients. Therefore, anti–CTLA-4 antibody has been combined with various other drugs to enhance its antitumor efficacy (6–10). One intriguing prospect for improving efficacy is to combine checkpoint inhibitors such as anti–CTLA-4 antibody, which target the adaptive immune system, with drugs targeting the innate immune system, seeking to evoke an additive or even synergistic immune response against the cancer. In this vein, innate immune receptors such as Toll-like receptors (TLRs) have great promise in cancer immunotherapy. For example, the TLR9 ligand CpG has been shown to have an antitumor effect in different cancers (11–13). Similarly, TLR7 agonist has been shown to reduce tumor burden in many different cancers, and the TLR7 agonist imiquimod is a Food and Drug Administration-approved drug for basal cell carcinoma (14–18). Other TLR ligands, including TLR2 ligand, have also been shown to have antitumor effects (19–24); some of these TLR agonists are currently in clinical trials (18).

Recent studies have challenged the idea that TLR ligands have only an adjuvant antitumor effect by their ligation to TLRs on innate immune cells in the host. For example, TLR1/2-mediated intrinsic signaling in tumor-specific T cells has been shown to increase the antitumor effect of T cells in a B16 melanoma model (23, 24). In addition, some studies suggested a T cell–intrinsic effect of TLR ligands like TLR2 ligands in reversing the immunosuppressive function of $CD4^+CD25^+$ Tregs (25, 26). TLR activation also provides costimulatory signals that promote T cell function and has been shown to increase IFN-γ and interleukin-2 production in T cells (23, 27–30).

Considering that TLR-mediated signaling can reverse the immunosuppressive function of Tregs and affect the modulation of adaptive immune responses directly or through dendritic cells (DCs) and macrophages, we hypothesized that TLR ligand synergizes with anti–CTLA-4 antibody to reduce tumor burden and that this combination treatment results in both the innate and adaptive components of the immune system attacking the tumor.

Significance

To overcome the challenge of nonresponsiveness or low effectiveness to current checkpoint blockade drugs, various combination therapies are under investigation for cancer treatment. In this study, we investigated a combination of Toll-like receptor 1/2 (TLR1/2) ligand and anti–CTLA-4 antibody in a mouse model of melanoma. TLR1/2 ligand enhanced the antitumor efficacy of anti–CTLA-4 by increasing Fcγ receptor IV expression, which in turn increased the depletion of tumor-infiltrating regulatory T cells. Whether ipilimumab causes Treg depletion in human patients is debatable; therefore, combining ipilimumab with Pam3CSK4 could lead to greater antitumor efficacy by introducing this modality. These findings are likely extensible to other checkpoint antibodies in cancer patients.

Author contributions: N.S. and J.P.A. designed research; N.S. performed research; J.V. contributed new reagents/analytic tools; N.S. and J.P.A. analyzed data; and N.S. and J.P.A. wrote the paper.

Conflict of interest statement: J.P.A. is an inventor and recipient of royalty from intellectual property licensed to Bristol-Meyers Squibb, Merck, and Jounce. He is a member of the scientific advisory board for Jounce Therapeutics, Neon Therapeutics, Amgen, Apricity, BioAtla, Forty-Seven, Tvardi Therapeutics, TapImmune, ImaginAb, Codiak Biosciences, and Marker Therapeutics. The authors have no other conflicting financial interests.

This article is a PNAS Direct Submission.

[1]To whom correspondence may be addressed. Email: nsharma1@mdanderson.org or jallison@mdanderson.org.

This article contains supporting information online at www.pnas.org/lookup/suppl/doi:10.1073/pnas.1819004116/-/DCSupplemental.

Published online May 10, 2019.

However, we surprisingly found that TLR1/2 ligand Pam3CSK4 enhances anti–CTLA-4-mediated tumor reduction through a unique mechanism; it increases FcγRIV expression on macrophages and thereby enhances depletion of Tregs.

Results

Pam3CSK4 Enhances the Antitumor Efficacy of Anti–CTLA-4 Antibody. In our initial approach to combine innate immune pathway modulation with anti–CTLA-4 treatment, we used heat-killed *Salmonella typhimurium* (HKST), which engages multiple TLRs, including TLR2, TLR4, and TLR5 (31–33), in combination with anti–CTLA-4 antibody. Mice were given an intradermal tumor challenge with B16/F10 and treated with anti–CTLA-4 antibody clone 9H10 with or without intratumoral injection of HKST (*SI Appendix*, Fig. S1*A*). Anti–CTLA-4 antibody alone did not significantly reduce tumor growth, but anti–CTLA-4 antibody plus HKST reduced tumor burden and increased survival (*SI Appendix*, Fig. S1*B*). We further treated B16/F10-challenged mice with the combination of anti–CTLA-4 plus Pam3CSK4, LPS, or Flagellin, which are ligands of TLR1/2, TLR4, and TLR5, respectively. The TLR1/2 ligand Pam3CSK4 most closely mimicked HKST's effects in reducing tumor burden and increasing survival in combination with anti–CTLA-4 (*SI Appendix*, Fig. S1*C*). To determine whether Pam3CSK4 can induce antitumor effects on its own or only in combination with anti–CTLA-4 antibody, B16/F10 tumor-challenged mice were injected with Pam3CSK4 intratumorally on different days with or without anti–CTLA-4 antibody. Compared with control mice given vehicle only, mice given Pam3CSK4 plus anti–CTLA-4 antibody, but not mice given Pam3CSK4 alone, had reduced tumor burden (Fig. 1 *A* and *B*) and increased survival (Fig. 1*B*). These results show that the antitumor effect of Pam3CSK4 plus anti–CTLA-4 combination is synergistic as Pam3CSK4 has no effects and anti–CTLA-4 has minimal effects as single agents on tumor burden and survival.

Due to the importance of immunological memory in immunotherapy, we sought to determine whether the combination treatment produces immunological memory in treated mice. We pooled combination-treated mice that survived primary tumor challenge and rechallenged them with a very high dose of the B16F/10 tumor without any further treatment. These mice completely cleared B16/F10 rechallenge and had 100% survival rate (Fig. 1*C*). To further confirm the systemic effects of combination therapy, we challenged mice bearing B16/F10 on both flanks and injected four doses of Pam3CSK4 into the right flank tumor in combination with i.p. injections of anti–CTLA-4 every 3 days beginning on day 3 after tumor challenge. We found that the combination of Pam3CSK4 and anti–CTLA-4 decreased tumor burden on distal tumor and significantly increased survival compared with single-agent treatment (Fig. 1*D*).

Pam3CSK4 Plus Anti–CTLA-4 Antibody Efficacy Depends on CD8 and CD4 T Cells. Both intratumoral CD8 and CD4 effector T cells have been shown to be involved with positive prognosis and improved disease-free survival in patients. To better understand the roles of these cell types in the therapeutic efficacy of Pam3CSK4 plus anti–CTLA-4 antibody, we performed tumor protection experiments with depleting antibodies or genetically deficient hosts. The therapeutic efficacy of Pam3CSK4 plus anti–CTLA-4 antibody was diminished in mice given CD8 T cell–depleting antibody (Fig. 2*A*). TLR2 is expressed by natural killer (NK) cells and B cells, which have been shown to be activated by TLR2 ligand to produce antitumor and antipathogen responses, respectively (34–36). Mice given NK cell- or B-cell–depleting antibodies did not have reduced combination treatment efficacy compared with mice not given these antibodies (Fig. 2*A*). Flow-cytometric analysis of peripheral blood from mice injected with depleting antibodies revealed that the antibodies were efficiently depleted their respective cell types (*SI Appendix*, Fig. S2). The therapeutic efficacy of the combination treatment was also diminished in mice lacking major histocompatibility complex class II molecules (Fig. 2*B*). These mice are devoid of CD4 T cells. Together, these results suggest that the efficacy of the combination treatment depends on CD8 and CD4 T cells, but not NK or B cells.

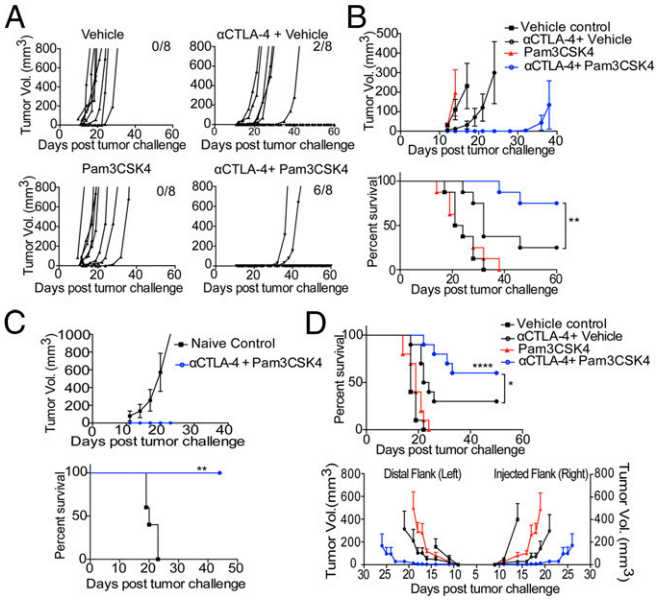

Fig. 1. Pam3CSK4 plus anti–CTLA-4 antibody enhances tumor rejection, increases survival, and produces immunological memory after B16/F10 tumor challenge. (*A*) Individual tumor growth, (*B*) average tumor growth (*Top*), and survival (*Bottom*) of mice in each treatment group. Mice were challenged with B16/F10 cells and given indicated treatments as described in *Materials and Methods*. Data are representative of three or four independent experiments with 5–10 mice per group. (*C*) Mice that survived primary B16/F10 challenge and had been earlier treated with combination therapy were rechallenged with 1.5×10^6 B16/F10 cells and left untreated. The black lines with squares represent the average tumor burden and survival of naive mice with no earlier tumor challenge or treatment, which served as a control. (*D*) Mice were challenged with B16/F10 cells on both flanks and were given indicated treatments as described in *Materials and Methods*. Intratumoral injections of Pam3CSK4 or Vehicle were given only on right flank. Survival (*Top*) and average tumor growth (*Bottom*) of mice in each treatment groups were monitored. Data are cumulative of two independent experiments with five mice per group. Error bars represent the mean ± SEM. $*P < 0.05$, $**P < 0.01$, and $****P < 0.0001$ (Mantel–Cox test).

We treated surviving mice from primary tumor challenge with CD8 T cell–depleting antibody or left them untreated before rechallenging with a high dose of B16F/10 tumor. Previously treated mice that were given CD8 T cell–depleting antibody were unable to clear tumor rechallenge and had 100% death rate (Fig. 2*C*). This suggested that CD8 T cells are indispensable for the immunological memory mediated protection in tumor-rechallenged mice.

Pam3CSK4 Plus Anti–CTLA-4 Antibody Enhances the Proinflammatory Function and Increases Granzyme B Expression of Antitumor Teffs. We next assessed the functional effect of combination treatment on tumor-infiltrating lymphocytes (TILs) and resident T cells in tumor-draining lymph nodes. To obtain enough TILs for the experiment, we delayed treatment; mice given a tumor challenge with B16/F10 received treatment on days 9 and 12. Two days after the last treatment, cells from tumors and tumor-draining lymph nodes were briefly restimulated ex vivo with B16/F10 antigen-loaded DCs and then analyzed for cytokine production

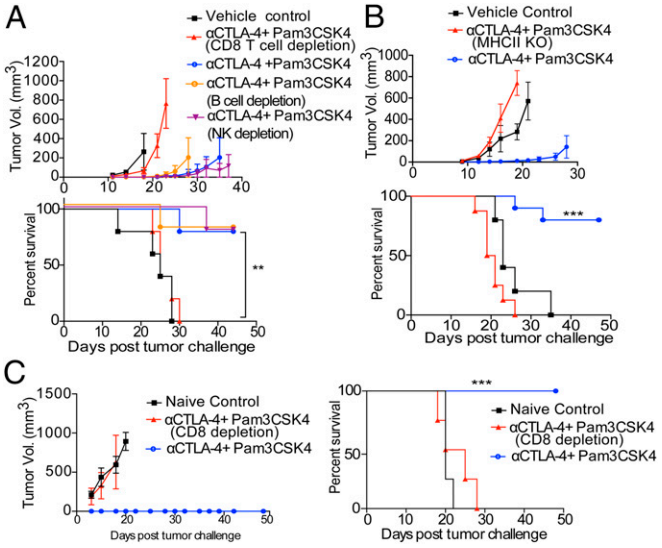

Fig. 2. Therapeutic efficacy of Pam3CSK4 plus anti–CTLA-4 antibody depends on CD4 and CD8 T cells in primary challenge and on CD8 T cells in rechallenge. (*A*) Average tumor growth (*Top*) and survival (*Bottom*) of mice that were challenged with B16/F10 cells and given the combination treatment and were also injected with anti-CD8 antibody (clone 2.4.3) for CD8 T cell depletion or anti-NK1.1 antibody (clone PK136) for NK cell depletion or anti-CD20 antibody (5D2) for B-cell depletion or were left untreated. Data are representative of two or three independent experiments with five to eight mice per group. (*B*) Average tumor growth (*Top*) and survival (*Bottom*) of MHC II KO mice and WT mice, which were challenged with B16/F10 cells and given combination therapy treatment. (*C*) Previously combination therapy-treated mice that survived primary B16/F10 challenge were either injected with anti-CD8 antibody (clone 2.4.3) for CD8 T cell depletion or left untreated. These mice were rechallenged with 1.5×10^6 B16/F10 cells, and tumor burden and survival of mice were monitored. Data are representative of two or three independent experiments with 5–10 mice per group. Error bars represent the mean ± SEM. $^{**}P < 0.01$ and $^{***}P < 0.001$ (Mantel–Cox test).

from T cells. Tumor-infiltrating CD8 T cells and CD4 Teffs from mice given the combination treatment had an increased frequency of IFN-γ producers compared with single treatment groups (Fig. 3*A*). The frequencies of IFN-γ–producing CD8 T cells and CD4 Teffs in the tumor-draining lymph nodes of mice were negligible in all treatment groups (Fig. 3*B*). TILs and T cells from tumor-draining lymph nodes were also activated with leukocyte activation mixture (BD Biosciences) containing phorbol myristate acetate (PMA)/ionomycin and, similar to activation with the B16/F10 antigen-loaded DCs, the frequencies of IFN-γ–producing CD8 T cells and CD4 Teffs in tumors were higher in the combination treatment group than in the single treatment groups (*SI Appendix*, Fig. S3 *A* and *B*). On the other hand, frequencies of IFN-γ–producing CD8 T cells and CD4 Teffs in the tumor-draining lymph nodes of mice given the combination treatment were not significantly different from those in the tumor-draining lymph nodes of mice given anti–CTLA-4 antibody alone (*SI Appendix*, Fig. S3 *C* and *D*). These data suggest that Pam3CSK4 plus anti–CTLA-4 antibody enhances the functions of only tumor-infiltrating CD8 T cells and CD4 Teffs but not draining lymph node resident T cells.

Compared with anti–CTLA-4 antibody alone, the combination treatment increased expression of granzyme B protein in both CD8 T cells and CD4 Teffs and increased the frequency of granzyme B-producing CD8 and CD4 Teffs in tumor (Fig. 3 *C* and *D*). Interestingly, the expression of granzyme B in CD8 and CD4 Teffs in tumor-draining lymph nodes and the frequencies of granzyme B-expressing CD8 and CD4 Teffs in the draining lymph nodes of mice given the combination treatment were not significantly different from those in the draining lymph nodes of mice given anti–CTLA-4 antibody alone (Fig. 3 *E* and *F*). Again, these results suggest that the functional effect of the combination treatment was limited to the tumor microenvironment.

Combination of Pam3CSK4 Plus Anti–CTLA-4 Antibody Enhances Treg Depletion and Increases CD8 T Cell/Treg and CD4 Teff/Treg Ratios Within the Tumor. As mentioned earlier, to obtain enough TILs to study the mechanism of the efficacy of combination treatment, we delayed treatment to days 9 and 12 after the tumor challenge. Even after delayed treatment, the tumors from mice given the combination treatment weighed significantly less than those from mice treated with anti–CTLA-4 antibody alone (*SI Appendix*, Fig. S4*A*). Furthermore, combination treatment was effective in reducing tumor burden and increasing survival compared with single treatments even if treatment was delayed and started at day 9 (*SI Appendix*, Fig. S4 *B* and *C*). To understand the effect of the combination therapy on the TIL population, we analyzed the frequency and density of each T cell subset within the tumor. The density of each subset was measured as the number of TILs per gram of tumor. The numbers of CD3 T cells and their percentage of the total $CD45^+$ population within tumor from mice given the combination treatment were significantly higher than those from mice given anti–CTLA-4 antibody alone (Fig. 4*A*). The number of tumor CD8 T cells and their percentage of the total T cells from mice given the combination treatment were also higher than those from mice given anti–CTLA-4 antibody alone (Fig. 4*B*). However, the percentages, but not the absolute numbers, of tumor CD4 T cells from mice given the combination treatment were smaller than those from mice given anti–CTLA-4 antibody alone (Fig. 4*C*). Despite its lack of effect on the density of tumor CD4 T cells compared with anti–CTLA-4 alone, the combination therapy increased the number of CD4 Teffs ($CD4^+FoxP3^-$ T cells) per gram of tumor and also increased the percentages of Teffs (Fig. 4*D*). We also analyzed intratumoral CD4Teff/Treg and CD8 T cells/Treg ratios because these ratios are predictive of therapeutic efficacy in the B16 melanoma model (4). We found that the CD4Teff/Treg ratios and CD8 T cells/Treg ratios from mice given the combination treatment were significantly higher than those from mice given anti–CTLA-4 antibody alone (Fig. 4*E*).

These findings that Pam3CSK4 plus anti–CTLA-4 antibody had no effect on the total number of intratumoral CD4 T cells despite increasing the population of CD4 Teffs compared with anti–CTLA-4 antibody alone raised the possibility that the combination treatment leads to an enhanced elimination of Tregs within tumors. Investigating this possibility, we found that mice given the combination treatment had significantly lower density of intratumoral Tregs than mice given anti–CTLA-4 antibody alone (Fig. 4*F*). The frequencies of Tregs within the CD4 T cell population were also reduced in mice given the combination treatment (Fig. 4*F*). Again, the percentages of different subsets of T cells including Tregs in draining lymph nodes did not differ significantly between different treatment groups, which suggests that the combination treatment's effect was tumor specific (*SI Appendix*, Fig. S5 *A* and *B*). Because Treg depletion is one of the mechanisms underlying the antitumor activity of anti–CTLA-4 antibody in some tumor models (5, 37), the finding that TLR1/2 stimulation enhanced anti–CTLA-4-mediated Treg depletion in the combination treatment group is quite interesting.

Enhanced Treg Depletion by Pam3CSK4 Plus Anti–CTLA-4 Antibody Is Dependent upon FcγRIV Expression. We analyzed mRNA extracted from tumors from mice treated with combination therapy of anti-CTLA-4 plus Pam3CSK4 and from mice given single anti-CTLA-4 treatment as reference by nanostring and Ingenuity Pathway Analysis (IPA). A number of genes was differentially up-regulated in the combination treatment group compared with single

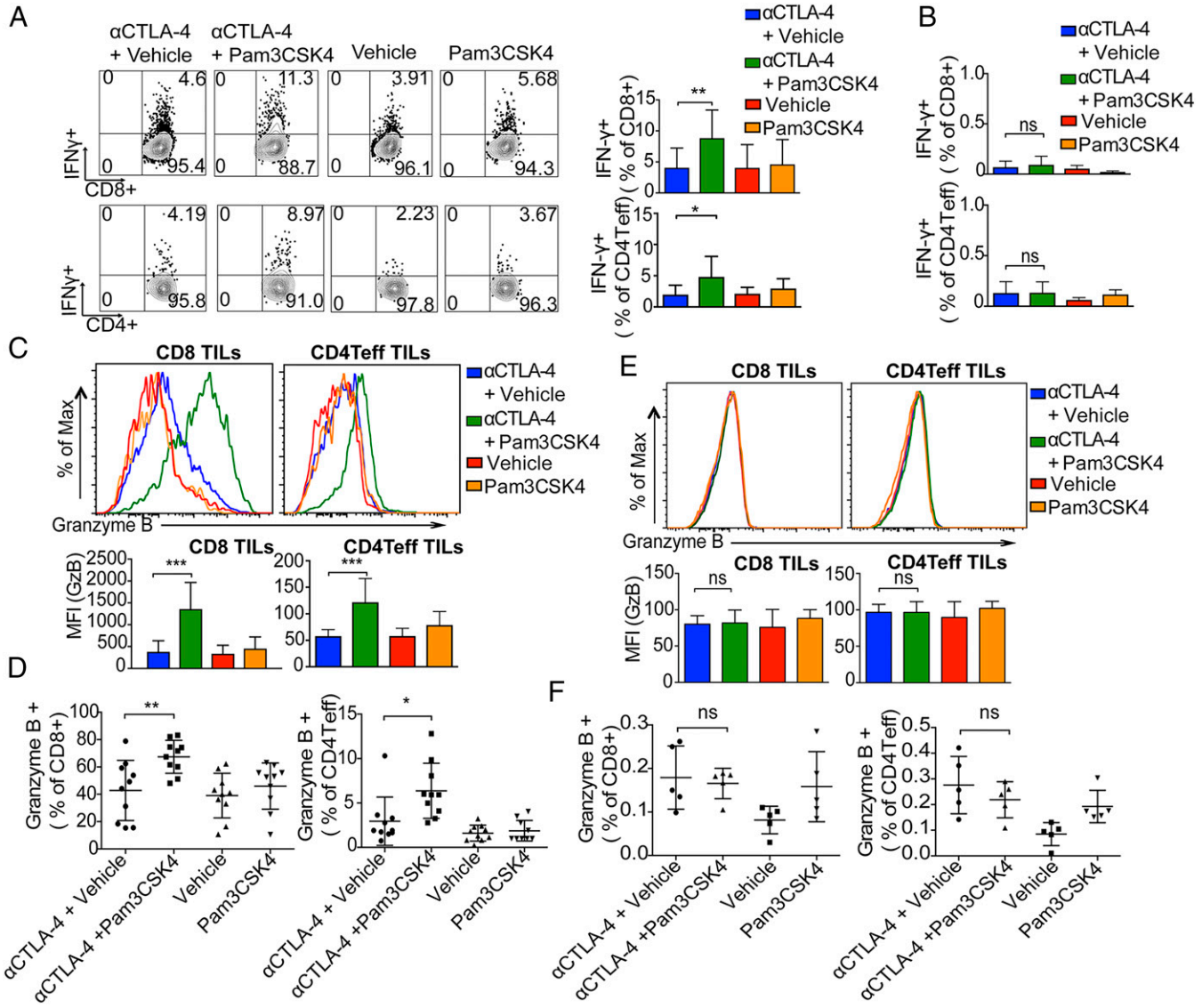

Fig. 3. Enhanced proinflammatory cytokine production and granzyme B expression in TILs by combination of Pam3CSK4 and CTLA-4 blockade. Mice were challenged with B16/F10 cells and given indicated treatments; tumors and dLNs cells were harvested, activated ex vivo with B16/F10 antigen-loaded DCs, and stained with indicated antibodies as described in *Materials and Methods*. (*A*) Representative flow cytometry plots and bar graphs of IFN-γ in CD8 T cells and CD4 Teff cells from TILs. Bar graphs show the cumulative frequencies of IFN-γ producers among tumor-infiltrating CD8 T cells and CD4 Teff from two of three independent experiments with five mice per group. (*B*) Bar graphs show the cumulative frequencies of IFN-γ producers among CD8 T cells and CD4 Teff in draining lymph nodes from two of three independent experiments with five mice per group. (*C*) Representative histogram plots (*Top*) and mean fluorescence intensity (MFI) plots (*Bottom*) of granzyme B staining of tumor-infiltrating CD8 T cells and CD4 Teffs. Data are representative of three or four experiments with five mice per group. (*D*) Cumulative frequencies of granzyme B^+ CD8 T cells and granzyme B^+ CD4 Teffs from two of three or four independent experiments with five mice per group. (*E*) Representative histogram plots (*Top*) and mean fluorescence intensity plot (*Bottom*) of granzyme B staining of draining lymph nodes' CD8 T cells and CD4 Teffs. Data are representative of three or four experiments with five mice per group. (*F*) Frequencies of granzyme B^+ CD8 T cells and CD4 Teffs among CD8 T cells and CD4 Teffs in draining lymph nodes. Data are representative of three or four experiments with five mice per group. Error bars represent the mean ± SD; ns, not significant; $*P < 0.05$, $**P < 0.01$, and $***P < 0.001$ (Student's *t* test).

anti-CTLA-4 treatment group (Fig. 5*A* and *SI Appendix*, Table S1). *SI Appendix*, Table S1 shows the 20 genes with most log2-fold change in the combination treatment group compared with the single antibody treatment group. Many of these genes are expressed in macrophages, and up-regulation of some of these genes or proteins is associated with antitumor phenotype. Functional analysis of the differentially expressed genes in the combination treatment group using IPA showed macrophage-related pathways among the top hit pathways (Fig. 5*B*). One of the genes up-regulated in the combination treatment group is Fcgr4, which we found interesting as we earlier showed that one of the mechanisms for Treg depletion by anti–CTLA-4 in some models is through FcγRIV-mediated antibody-dependent cell-mediated cytotoxicity (ADCC) by macrophages (5). Considering that we see increased depletion of Tregs in the combination treatment group compared with the single antibody treatment group, we further looked at the expression of FcγRIV by flow cytometry. Interestingly, compared with anti–CTLA-4 antibody alone, the combination treatment of anti-CTLA-4 plus Pam3CSK4 as well as Pam3CSK4 alone increased expression of FcγRIV on tumor-associated macrophages (TAMs) (Fig. 6*A*) but not on draining lymph node resident macrophages (*SI Appendix*, Fig. S5*C*).

We further analyzed the role of FcγRIV expression in combination treatment efficacy using FcγRIV knockout (KO) mice.

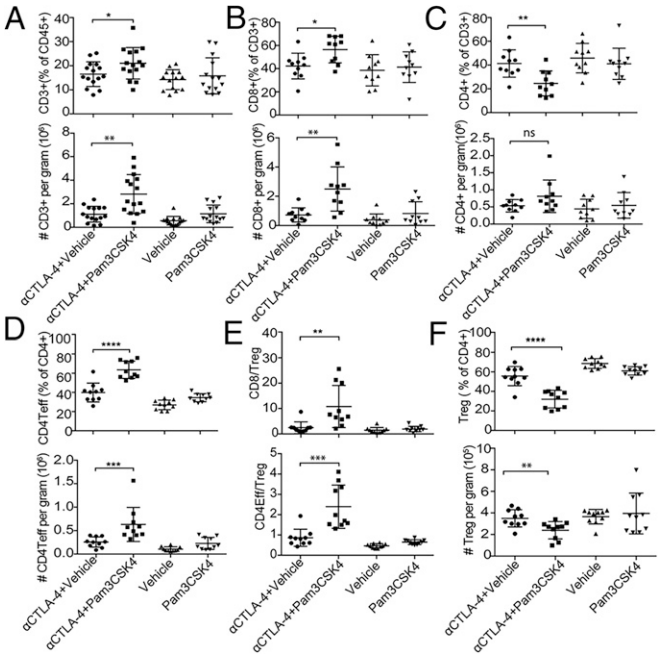

Fig. 4. Combination of Pam3CSK4 and CTLA-4 blockade enriches CD8 T cells, depletes Treg, and increases the CD8/Treg and CD4 Teff/Treg ratios in tumor microenvironment. Mice were challenged with B16/F10 cells and were given indicated treatments; cells from tumors were harvested and stained with indicated antibodies as described in *Materials and Methods*. (*A*–*D*) (*Top*) Cumulative frequencies of CD3 T cells as percentages of $CD45^+$ cells (*A*), CD8 T cells as percentages of $CD3^+$ T cells (*B*), CD4 T cells as percentages of $CD3^+$ T cells (*C*), CD4 Teffs as percentages of CD4 T cells (*D*), and (*Bottom*) these cell types' respective densities as the cumulative absolute numbers of the cells per gram of tumor from two to three of four independent experiments. (*E*) Intratumoral CD8/Treg and CD4 Teff/Treg ratios on day 14 in each group. (*F*, *Top*) Cumulative frequencies of $CD4^+FoxP3^+$ Tregs as the percentages of CD4 T cell from two to three of four independent experiments. (*F*, *Bottom*) Density of $CD4^+Foxp3^+$ Tregs as a cumulative absolute number of cells per gram of tumor from two of four independent experiments. Error bars represent the mean ± SD; ns, not significant; $^*P < 0.05$, $^{**}P < 0.01$, $^{***}P < 0.001$, and $^{****}P < 0.0001$ (Student's *t* test).

The antitumor effects of anti-CTLA-4 plus Pam3CSK4 combination treatment were considerably diminished in the absence of FcγRIV expression in mice, further confirming role of FcγRIV in combination treatment efficacy (Fig. 6*B*). The anti–CTLA-4 plus Pam3CSK4 treatment-induced decrease in regulatory T cell frequencies that we observed in wild-type (WT) mice did not occur in FcγRIV KO mice (Fig. 6*C*). The increase in CD8 T cells to Treg ratio and CD4 Teff to Treg ratio as well as GzB^+ CD8T cells to Treg ratio in combination treatment observed in WT mice was also significantly reduced in FcγRIV KO mice (Fig. 6*D*). We evaluated the efficacy of combination treatment to induce IFN-γ secretion from CD8 T cells in FcγRIV KO mice by ex vivo activation of TILs with BD leukocyte activation mixture containing PMA/ionomycin. The combination treatment did not increase IFN-γ secretion from CD8 T cells in FcγRIV KO mice (Fig. 6*E*).

We showed earlier by using surface plasmon resonance analysis that unlike the 9H10 clone of anti–CTLA-4, which is a Syrian hamster IgG2b, the Armenian hamster IgG1 clone 4F10 of anti–CTLA-4 does not show any appreciable binding to FcγRIV (5). Therefore, to confirm the importance of FcγRIV-mediated Treg depletion in Pam3CSK4 plus anti–CTLA-4 antibody (9H10 clone) combination therapy efficacy, we treated tumor-bearing mice with Pam3CSK4 plus 4F10. We found that Pam3CSK4 did not enhance efficacy of 4F10 in decreasing tumor burden or in increasing survival rate of mice against B16/F10 tumor challenge (Fig. 6*F*). We also found that the frequencies of Treg, CD4 Teff, and GzB^+CD8 T cell population in mice treated with combination of 4F10 plus Pam3CSK4 after B16/F10 challenge were not significantly different from 4F10 single treatment (Fig. 6*G*). We also found that 4F10 plus Pam3CSK4 combination treatment did not enhance frequencies of IFN-γ^+CD8^+ T cells and IFN-γ^+ CD4 Teffs compared with 4F10 single treatment (Fig. 6*H*). These experiments provided additional support for the model that FcγRIV has a significant role in anti–CTLA-4 antibody (9H10) plus Pam3CSK4 combination treatment efficacy.

FcγRIV does not exist in humans, although FcγRIIIA can be considered a human functional homolog to mouse FcγRIV. Furthermore, in contrast to 9H10, which is a Syrian hamster IgG2b, ipilimumab is a fully human IgG1 antibody and interacts with human FcγRIIIA. Also, ipilimumab does not appear to deplete $FoxP3^+$ regulatory T cells (Tregs) in human cancers (38).

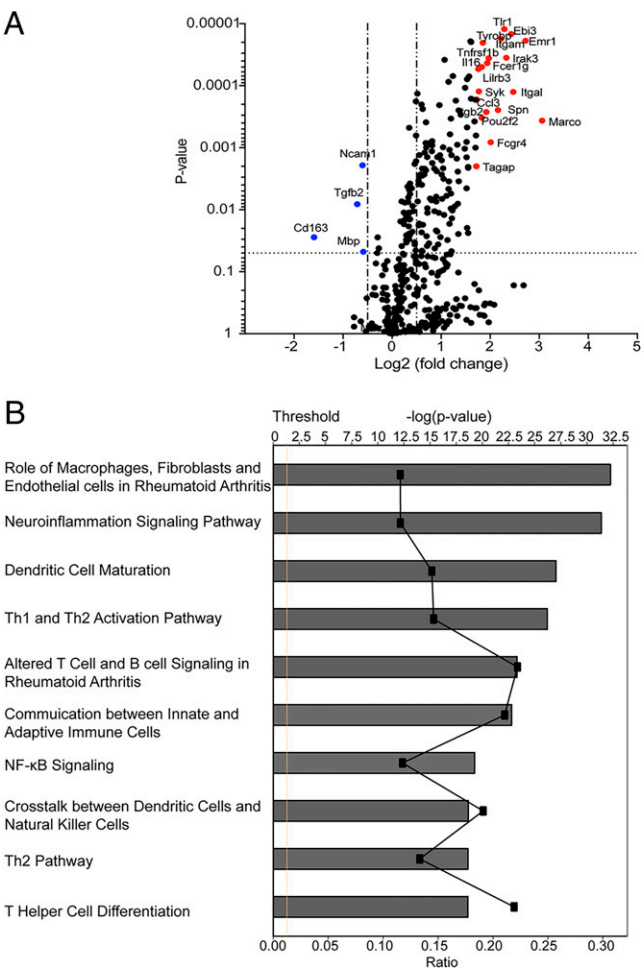

Fig. 5. Differential expression of macrophage-specific genes and pathway in combination treatment compared with anti-CTLA-4 antibody control. (*A*) Differential gene expression profiling was performed by Nanostring analysis. Volcano plot was made in Prism and illustrates the log2-fold change in gene expression (anti-CTLA-4+Pam3CSK4 vs. anti-CTLA-4) on the *x* axis and *P* values on the *y* axis. Top 20 up-regulated genes are colored red, and down-regulated genes are in blue. (*B*) Graph shows category scores and 10 most up-regulated pathways, which were determined by IPA "Core analysis." Ratio refers to the number of molecules from the dataset that map to the pathways listed divided by the total number of molecules that define the canonical pathway from within the IPA knowledgebase. Threshold (dotted line) is set at 1.3 and indicates the minimum significance level, which is scored as −log(*P* value) from Fisher's exact test.

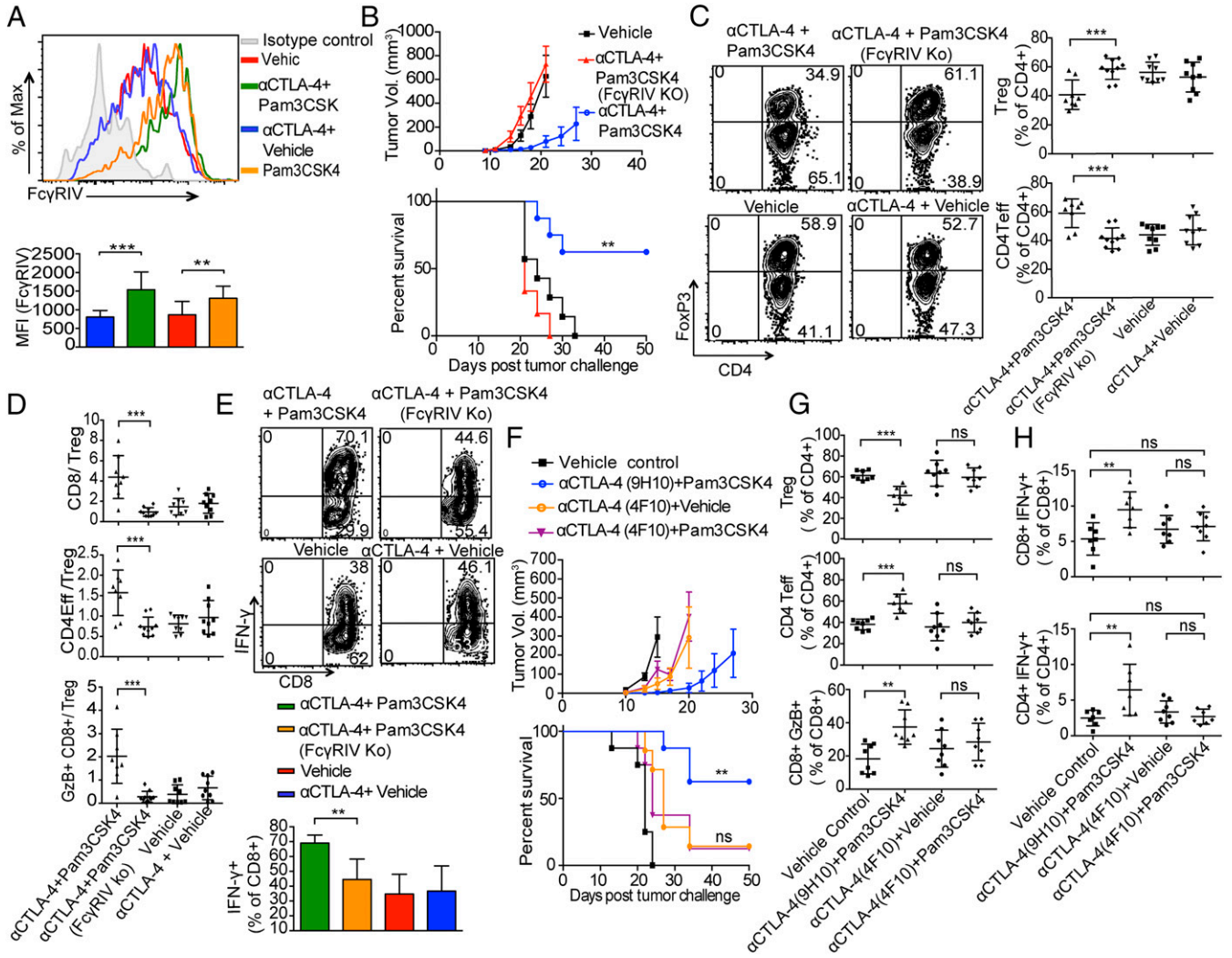

Fig. 6. FcγRIV is essential for the efficacy of Pam3CSK4 plus anti–CTLA-4 antibody and its expression on macrophages is enhanced by Pam3CSK4. (*A*) Representative flow histogram plot (*Top*) and mean fluorescence intensity bar graph (*Bottom*) of FcγRIV expression on $CD11b^+GR1^-F\text{-}4/80^+$ TAMs from B16/F10-challenged mice given treatments as indicated. Data are representative of three or four independent experiments with four or five mice per group. Error bars represent the mean ± SD. (*B*) Average tumor growth (*Top*) and survival (*Bottom*) of mice in WT or FcγRIV KO hosts that were challenged with B16/F10 cells and were given combination therapy treatments. Data are representative of two or three independent experiments with five to eight mice per group. Error bars represent the mean ± SEM. $^{**}P < 0.01$ (Mantel–Cox test). (*C* and *D*) WT and FcγRIV KO mice were challenged with B16/F10 cells and were given indicated treatments; cells from tumors were harvested and stained as described in *Materials and Methods*. (*C*) Representative flow cytometry plots and frequencies of $CD4^+FoxP3^+$ Tregs and $CD4^+FoxP3^-$ CD4Teff as the percentages of CD4 T cells (*D*) CD8 T cells, CD4 Teff, and GzB^+ CD8 T cells to Treg ratio. Data are cumulative of two experiments of three independent experiments with four to five mice per group. (*E*) Mice were challenged with B16/F10 cells and were given indicated treatments, tumors were harvested, activated ex vivo with BD leukocyte activation mixture, and stained with indicated antibodies as described in *Materials and Methods*. Representative flow cytometry plots and cumulative frequencies of IFN-γ producers among tumor-infiltrating CD8 T cells from two of three independent experiments with four to five mice per group. Error bars represent the mean ± SD. (*F*) Average tumor growth (*Top*) and survival (*Bottom*) of mice challenged with B16/F10 cells and given indicated treatments. Error bars represent the mean ± SEM. $^{**}P < 0.01$ is significance between anti–CTLA-4 (9H10)-plus-Pam3CSK4 vs. vehicle control group, whereas ns is not significant and measured between anti–CTLA-4 (4F10)-plus-vehicle vs. anti–CTLA-4 (4F10)-plus-Pam3CSK4 group (Mantel–Cox test). (*G*) Mice were challenged with B16/F10 cells and given treatments as indicated; cells from tumors were harvested and stained with indicated antibodies as described in *Materials and Methods*. Cumulative frequencies of $CD4^+Foxp3^+$ Tregs, $CD4^+Foxp3^-$ Teff cells and $CD8^+GzB^+$ T cells from two of three independent experiments with three to five mice per group. (*H*) Mice were challenged with 6×10^5 B16/F10 cells and were given two doses of treatments as indicated on day 9 and 12 after tumor challenge. Cells from tumors were harvested at day 14 after tumor challenge, activated ex vivo with B16/F10 antigen-loaded DCs, and stained with indicated antibodies as described in *Materials and Methods*. Scatter dot plots show cumulative frequencies of IFN-γ producers among tumor-infiltrating CD8T cells (*Top*) and CD4 Teffs cells (*Bottom*) from two of three experiments with three to five mice per group. Error bars represent the mean ± SD; ns, not significant; $^{**}P < 0.01$ and $^{***}P < 0.001$ (Student's *t* test).

However, ipilimumab has been shown to mediate ex vivo ADCC of Tregs by monocytes through FcγRIIIA, and Arce Vargas et al. (39, 40) in humanized mouse model showed that the activity of human anti–CTLA-4 depends at least partially on depletion of Tregs. Therefore, we wanted to know whether expression levels of FcγRIII can also be modulated by Pam3CSK4 on human $CD11b^+$ cells. We activated healthy human PBMCs with Pam3CSK4 in vitro and analyzed expression of FcγRIII by flow cytometry. We found that Pam3CSK4 increased FcγRIII expression on human $CD11b^+$ cells (*SI Appendix*, Fig. S6).

Macrophages Are Essential for the Efficacy of Combination Therapy of Pam3CSK4 Plus Anti–CTLA-4 Antibody. Compared with anti–CTLA-4 antibody alone, the combination treatment increased not only expression of FcγRIV on macrophages but also the density of macrophages in the tumor microenvironment (Fig. 7*A*). To assess

the role of macrophages in the efficacy of the combination treatment, mice were challenged with B16/F10 and were also injected with clodronate liposomes to deplete macrophages. The efficacy of the combination treatment in decreasing tumor burden and increasing survival rate was diminished in macrophage-depleted mice (Fig. 7*B*). The other cell type that expresses FcγRs are NK cells; mice depleted of NK cells show no defect in combination treatment efficacy (Fig. 2*A*).

Macrophages can be assigned M1 or M2 phenotype depending upon expression of certain receptors and their proinflammatory or antiinflammatory functions (41). M1 macrophages are considered to have a protective role against tumors, whereas M2 macrophages have protumor effects. As TLR ligands can tip the M1–M2 balance toward M1 macrophages, we assessed the phenotypes of macrophages in the tumor microenvironment in mice given different treatments. Inducible nitric oxide synthase (iNOS) is one of the signature molecules expressed by M1 macrophages and is important for its antitumor function; therefore, we considered $CD11b^{+}GR1^{-}F\text{-}4/80^{+}MHCII^{+}iNOS^{+}$ macrophages as M1 macrophages for our assessment. Our data show an increase in frequency and total numbers of M1 macrophages in combination-treated mice. (Fig. 7 *C* and *D*). We did not see such increase in M1 macrophage frequency or number with TLR1/2 ligand Pam3CSK4 alone. As IFN-γ is known to skew macrophages to M1 phenotype, this could be a result of increased IFN-γ secretion by T cells in combination treatment compared with other single treatments (Fig. 3*A*). M1 skewing in combination treated tumor microenvironment could also be an effect of loss of Treg cells as some studies suggest that Treg cells can control numbers of inflammatory monocytes either by preventing their recruitment and/or differentiating monocytes toward M2 macrophages (42, 43).

TLRs have been shown to directly costimulate T cell functions and modulate the immunosuppressive functions of Tregs (26, 28). To determine whether the TLR1/2 ligand directly affects T cells in mice given the combination treatment, we assessed tumor burden and survival with $MyD88^{Flox/Flox}$ CD4 Cre^{+} mice, which do not have MyD88, an adaptor molecule involved in downstream TLR signaling in T cells. The absence of MyD88 in T cells did not significantly affect the efficacy of the combination treatment against B16/F10 tumor challenge (Fig. 7*E*). We also did an experiment with $MyD88^{Flox/Flox}$ $CD11bCre^{+}$ mice as macrophages express CD11b; we expected to have no MyD88 signaling in macrophages in these mice. The combination treatment was completely ineffective in these mice (Fig. 7*F*). We analyzed intratumoral Treg frequencies in $MyD88^{Flox/Flox}$ $CD11bCre^{+}$ mice challenged with B16F10 and treated with combination treatment; our results suggest that combination treatment was ineffective in decreasing intratumoral Treg frequencies in $MyD88^{Flox/Flox}$ $CD11bCre^{+}$ mice compared with

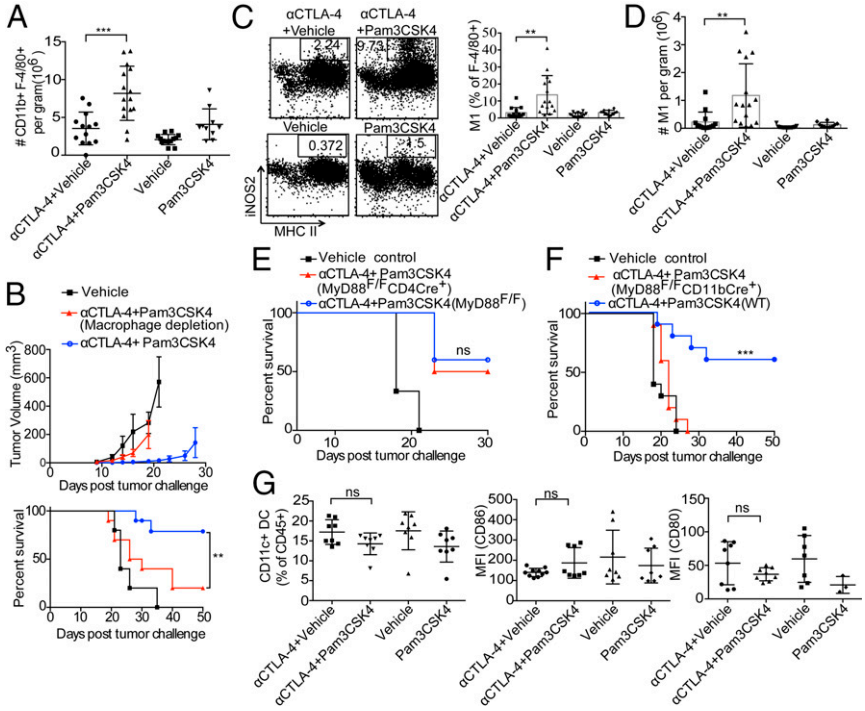

Fig. 7. Pam3CSK4 plus anti–CTLA-4 antibody efficacy is dependent upon macrophages. (*A*) Mice were challenged with B16/F10 cells and given treatments; cells from tumors were harvested and stained with antibodies. Macrophage density as a cumulative absolute number of $CD11b^{+}GR1^{-}F\text{-}4/80^{+}$ cells per gram of tumor from three or four independent experiments with four to five mice per group. (*B*) Average tumor growth (*Top*) and survival (*Bottom*) of mice given combination treatment after B16/F10 challenge and that did or did not receive clodronate liposomes for macrophage depletion. Error bars represent the mean ± SD. $^{**}P < 0.01$ (Mantel–Cox test). (*C*) Representative dot plots and cumulative frequencies of M1 macrophages. Cumulative frequencies of M1 macrophages from three independent experiments were calculated as the percentages of $CD11b^{+}GR1^{-}F\text{-}4/80^{+}$ macrophages. (*D*) M1 macrophage density as a cumulative absolute number of cells per gram of tumor from three independent experiments with four to five mice per group. (*E*) Average survival of $MyD88^{Flox/Flox}$ $CD4Cre^{+}$ and (*F*) $MyD88^{Flox/Flox}$ $CD11bCre^{+}$ mice, which were challenged with B16/F10 cells and given combination therapy treatment. Data are representative of two experiments with four to five animals per group. ns, not significant; $^{***}P < 0.001$ (Mantel–Cox test). (*G*) Cumulative frequencies of $CD11b^{-}Gr\text{-}1^{-}F\text{-}4/80^{-}CD11c^{+}$ cells of live $CD45^{+}$ cells and mean fluorescence intensity (MFI) of CD86 and CD80 from two independent experiments with three to five mice per group. Mice were challenged with 6×10^{5} B16/F10 cells and were given two doses of treatments as indicated on day 9 and 12 after tumor challenge. Cells from tumors were harvested at day 14 after tumor challenge and stained with indicated antibodies as described in *Materials and Methods*. Error bars represent the mean ± SEM; ns, not significant; $^{**}P < 0.01$ and $^{***}P < 0.001$ (Student's *t* test).

vehicle-injected control mice (*SI Appendix*, Fig. S7). These results confirm an important role of CD11b$^+$ cells and hence macrophages in combination treatment efficacy. We assessed the role of DCs in the efficacy of combination treatment by analyzing frequencies and activation of CD11c$^+$ DCs. We found no difference in frequencies of CD11c$^+$ DCs or expression of activation markers like CD80 and CD86 between single anti–CTLA-4 and combination treatment groups (Fig. 7*G*), suggesting that DCs do not play major role in combination treatment efficacy in our model.

Pam3CSK4 Plus Anti–CTLA-4 Antibody Has Protection Efficacy in Multiple Tumor Models. To determine whether the combination of Pam3CSK4 plus anti–CTLA-4 antibody has efficacy in multiple tumor models, we used the mT5 mouse model of pancreatic cancer (44). As in the B16/F10 tumor model, Pam3CSK4 plus anti–CTLA-4 antibody reduced tumor volume and provided a statistically significant survival benefit (Fig. 8 and *SI Appendix*, Fig. S8). Treatment with anti–CTLA-4 antibody or Pam3CSK4 alone had no significant effect on tumor reduction or survival. These results suggest that the combination treatment is also effective in the treatment of mT5, which does not respond to anti–CTLA-4 therapy alone. We observed that mice given the combination treatment had significantly lower frequencies of intratumoral Tregs than mice given anti–CTLA-4 antibody alone (*SI Appendix*, Fig. S9*A*). The density of Tregs was also reduced in mice given the combination treatment (*SI Appendix*, Fig. S9*B*). We also found that the CD4Teff/Treg ratios from mice given the combination treatment were significantly higher than those from mice given anti–CTLA-4 antibody alone (*SI Appendix*, Fig. S9*C*). This further confirms that combination treatment enhances antitumor efficacy by increasing depletion of intratumoral regulatory T cell population. This mechanism is not specific to one tumor model.

Discussion

Our findings indicate that the TLR1/2 ligand Pam3CSK4 enhances the antitumor efficacy of anti–CTLA-4 antibody. They also indicate a unique mechanism by which Pam3CSK4 enhances FcγRIV expression on macrophages, which plays a role in mediating the effects of the combination treatment by supporting ADCC-mediated depletion of Tregs coated with anti–CTLA-4 antibodies. These findings have major implications for cancer immunotherapy, as recent studies have demonstrated the importance of Fc receptors in the anticancer efficacy of various checkpoint inhibitors (5, 37, 45–47).

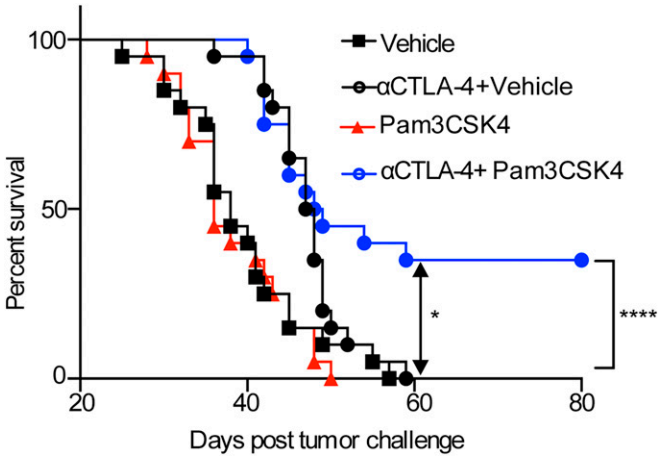

Fig. 8. Pam3CSK4 plus anti–CTLA-4 antibody has therapeutic efficacy against mouse pancreatic tumor model. Survival of mice in each treatment group. Mice were challenged with 1×10^5 mT5 cells and were given indicated treatments. Data are cumulative of three independent experiments with five to seven mice per group. *$P < 0.05$ is significance between anti–CTLA-4-plus-vehicle vs. anti–CTLA-4-plus-Pam3CSK4 group, whereas ****$P < 0.0001$ is significance between vehicle control vs. anti–CTLA-4-plus-Pam3CSK4 group (Mantel–Cox test).

While we previously showed that antibodies to CTLA-4 enhance tumor cell killing by a T effector cell-intrinsic mechanism (48), the findings of the present study are consistent with those of our earlier studies in a mouse model of B16 melanoma expressing GM-CSF, which showed that Treg depletion is an additional mechanism by which anti–CTLA-4 antibody has antitumor function. They also agree with our earlier findings that FcγRIV expression on macrophages is important for the anti–CTLA-4 plus GM-CSF–mediated depletion of Tregs (5). Our findings of intratumoral depletion of Tregs in combination therapy agree with recently reported studies showing that the TLR-9 ligand CpG combined with anti–CTLA-4 and anti-OX40 antibodies increased antitumor therapeutic efficacy due to the depletion of tumor-infiltrating Tregs in a lymphoma model (49). As a result of these studies showing that the antitumor antibodies used in targeting Teff cells may have both direct effects on Teff cells as well as FcγR-mediated depletion of Tregs, there is an increased interest in developing antibodies that can support both modalities.

In our studies, the functional efficacy of TLR1/2 ligand in enhancing anti–CTLA-4 antibody-mediated depletion of regulatory T cells and in increasing IFN-γ secretion from T cells was specific for the tumor microenvironment as we did not see such effects in tumor draining lymph nodes. This could be due to a lower number of macrophages in the draining lymph nodes as well as lack of increase of FcγRIV expression on draining lymph node macrophages in combination treatment, which might be below the threshold need for depletion of Tregs (*SI Appendix*, Fig. S5*C*). In addition, it has been shown that TLR1/2 ligand has an antitumor effect in a B16 model, and that this effect is intrinsic to T cells (23, 24). Unlike those findings, we did not find that TLR1/2 ligand by itself had an effect on tumor burden. Moreover, our data from experiments with MyD88$^{Flox/Flox}$ CD4 Cre$^+$ mice did not suggest that Pam3CSK4 had a T cell–intrinsic role in the efficacy of the combination treatment. These differences could be attributed to the possibility that TLR1/2 ligand has a reduced T cell–intrinsic effect on the endogenous T cell population but has a more pronounced effect on large numbers of adoptively transferred transgenic antigen-specific T cells, which were used in the above-mentioned studies. The cross talk between TLR receptor and Fc receptor signaling during bacterial infection has been shown earlier (50), and TLR2 receptor has also been shown to be involved in DC dysfunction by regulating IL-6 and IL-10 receptor signaling (51). Considering TLR1/2 ligand alone did not have any effect on tumor burden or Treg population when injected alone and also no change in expression of CD80 or CD86 on CD11c$^+$ DCs in combination treatment, we can rule out these mechanisms and increased Treg depletion by Pam3CSK4 plus anti–CTLA-4 antibody seems to be the primary mechanism in our model. The differences that we see in Pam3CSK4 effects on DCs in our studies compared with above-mentioned studies could be due to the use of different models; the previous study used GVAX tumor model and also adoptively transferred OT-I–specific CD8 T cells in the B16-Ova model.

In this study, we show that TLRs can modulate the expression of Fcγ receptors on macrophages and increase the antitumor efficacy of anti–CTLA-4 antibody treatment. This increase in antitumor efficacy could be due to an increased antibody binding to the FcγRIV or due to the increase in ADCC activity of macrophages. We did an experiment with the 4F10 clone of anti–CTLA-4 antibody, which is less efficient in binding to murine FcγRIV. This antibody fails to have antitumor effect in combination with TLR1/2 ligand. We also show that FcγRIV is important

for the efficacy of combination treatment by using FcγRIV KO mice. Together, these data suggest an importance of binding efficacy of anti–CTLA-4 antibody to FcγRIV for enhanced ADCC of Treg in our model in combination treatment group. It still does not rule out the possibility of enhanced ADCC activity of macrophages due to another mechanism. These findings have major implications for the treatment of patients with poorly immunogenic tumors, which are less responsive or are resistant to checkpoint inhibitors, including ipilimumab. Combining a checkpoint blockade antibody like anti–CTLA-4 with TLR1/2 ligand, which can have an impact on the tumor microenvironment, could change the clinical outcome of such patients.

As stated earlier, despite functional similarities between murine and human FcγRs, these receptors also have some differences. Therefore, our findings in mouse models of cancer in the present study need to be studied for relevance in human cancer patients. In any event, our findings of increase in FcγRIII expression on human $CD11b^+$ cells in vitro by Pam3CSK4 stimulation suggested a possibility of potential of increased depletion of Tregs and hence increased efficacy by anti–CTLA-4-plus-Pam3CSK4 therapy in human patients by a mechanism similar to that which we demonstrated. It is important to mention that, while we did not see depletion of regulatory T cells by ipilimumab in patients, that leaves a gap for potential improvement of functioning of ipilimumab by increasing Treg depletion efficacy of ipilimumab. There are efforts underway at several pharmaceutical companies to engineer the Fc region of ipilimumab to enhance FcR binding and consequently increase depletion of Tregs.

Although our studies are limited to only anti–CTLA-4 antibodies, our results suggest a possibility that TLR1/2 ligands could have a positive impact on final outcome if combined with other immunotherapy antibodies such as anti–OX-40, anti-ICOS, or anti-GITR that are also highly expressed on tumor-infiltrating Treg cells. Treg depletion has also been demonstrated with antibodies against some of these receptors (40). Our findings show that combining TLR1/2 ligand with anti–CTLA-4 antibody is a promising approach to cancer treatment and that TLR1/2 ligand enhances FcγRIV expression, which can be used to modulate the efficacy of other antibody-based immunotherapies.

Materials and Methods

Mice. Six- to 8-wk-old C57BL/6 WT mice and MHC class II KO mice (Δ78) were purchased from The Jackson Laboratory. FcγRIV KO mice were obtained from Dr. J. V. Ravetch (The Rockefeller University, New York, NY). To generate $MyD88^{Flox/Flox}$ $CD4\ Cre^+$ mice and $MyD88^{Flox/Flox}$ $CD11b\ Cre^+$, we crossbred $MyD88^{Flox/Flox}$ mice with CD4Cre and CD11b Cre mice, respectively (52). All mice were housed under specific pathogen-free conditions in accordance with institutional guidelines. MD Anderson Cancer Center's Institutional Animal Care and Use Committee approved all animal experiments.

Cell Lines and Reagents. The mouse melanoma cell line B16/F10 was obtained from Dr. Isaiah Fidler (MD Anderson Cancer Center, Houston, TX) and maintained as described previously (53). The pancreatic cancer cell line mT5 was obtained from Dr. David Tuveson (Cold Spring Harbor Laboratory, Cold Spring Harbor, NY) and maintained as described previously (44). Anti–CTLA-4 antibody (clone 9H10 and clone 4F10) was purchased from BioXCell and administered intraperitoneally. Pam3CSK4, LPS, and HKST were purchased from Invivogen, whereas Flagellin was purchased from Novus Biologicals and injected intratumorally. Ribopure RNA purification kit was purchased from Thermo Fisher Scientific. GentleMACS M tubes were purchased from Miltenyi Biotec. Clodronate liposomes were purchased from www.clodronateliposomes.org. In vivo depletion antibodies such as anti-CD8 (clone 2.43) and anti-NK1.1 (clone PK136) were purchased from BioXcell. Anti-CD20 antibody (clone 5D2) was a gift from Dr. Andrew C. Chan (Genentech, South San Francisco, CA). The following antibodies were used for flow cytometry analysis of tumors and draining lymph nodes. Anti-CD4 (clone GK1.5), anti-CD8 (clone 53-6.7), anti-CD45.2 (clone 104), anti-F4/80 (clone BM8), anti-FcγRIV (clone 9E9), anti-TNFα (clone MP6 XT22), anti-B220 (clone RA3-6B2), and anti–I-A/I-E (clone M5/114.15.2) were purchased from Biolegend. Anti-CD3 (clone 145-2C11), anti-granzyme B (clone GB11), anti–IFN-γ (clone XMG1.2), and anti-CD64 (clone X54-5/7.1) were purchased from BD Biosciences. Anti-Foxp3 (clone FJK-16s), anti-CD11b (clone M1/70), anti-iNOS (clone CXFNT), anti-hCD11b (clone ICRF44), and anti–GR-1 (clone 1A8) were purchased from eBioscience. Anti-hCD16 antibody was purchased from BD Biosciences.

In Vivo Depletion Assays. Mice were given i.p. injections of CD8 depletion antibody (clone 2.43; initial dose, 500 μg), NK cell depletion antibody (clone PK136; initial dose, 600 μg), and B-cell depletion antibody (anti-CD20; clone 5D2; initial dose, 400 μg) on the day of tumor challenge (day 0); depletion was maintained with injections of the antibodies at half their initial doses on days 3, 6, 9, and 12. For macrophage depletion, clodronate liposomes (200 μL) were injected on the day of tumor challenge and then injected on days 3, 6, 9, and 12. For the immunological memory experiment, anti-CD8 depletion antibody was given at an initial dose of 500 μg 3 days before tumor rechallenge and then given at half its initial dose on days 0 (the day of tumor rechallenge), 3, and 6. Depletion by different antibodies was assessed by analyzing respective cell populations in peripheral blood by flow cytometry 2 days after the last injections and comparing it with untreated control. For this end, peripheral blood was collected from the tail veins of mice from each group. Red blood cells were lysed with RBC lysing buffer (Sigma-Aldrich), and lymphocytes were filtered through cell strainers. Cells were stained with the indicated antibodies and analyzed by flow cytometry.

Tumor Challenge and Treatment. Mice were given intradermal injections of 3×10^5 B16/F10 cells or s.c. injections of 1×10^5 mT5 cells on their right flanks on day 0. Mice were then treated with i.p. injections of anti–CTLA-4 antibody (clone 9H10 or clone 4F10; 100 μg) and intratumoral injections of TLR ligands (Pam3CSK4, 10 μg/ea; Flagellin, 10 μg/ea; LPS, 10 μg/ea) or HKST (10^9 cells/ea) on days 3, 6, 9, and 12. The anti–CTLA-4 antibody dose was doubled on day 3. For experiments to look at systemic effects of treatment, mice were challenged on both flanks with intradermal injections of 3×10^5 B16/F10 cells, intratumoral injections of Pam3CSK4 or vehicle were given only on the right flank. For rechallenged memory experiments, mice that survived primary B16/F10 challenge and had been earlier treated with combination therapy were rechallenged with 1.5×10^6 B16/F10 cells and left untreated. In experiments in which mice would be killed on day 14, injections of anti–CTLA-4 antibody and TLR ligands were given on days 9 and 12 only. In these experiments, the initial injection of B16/F10 cells was doubled to 6×10^5 cells. These mice were killed on day 14 to obtain tumors and draining lymph nodes or to analyze tumor growth. For the tumor burden or survival experiments, the mice were considered moribund when the tumor grew to 1,000 mm^3 and humanely killed.

Tumor Processing and Flow Cytometry. For phenotypic and functional analysis of tumor-infiltrating cells, mice were challenged and treated as described above. Mice from each treatment group were humanely killed on day 14, and their tumors and tumor-draining lymph nodes were isolated. Isolated tumors were weighed, mechanically dissected, and then digested with Dnase I and Liberase TL (Roche) at 37 °C for 30 min and then filtered through 70-μm nylon cell strainer. Lymph nodes were mechanically dissected through a 70-μm nylon cell strainer and washed. These cells were stained with Live/Dead fixable blue (Life Technologies) to exclude dead cells from analysis before staining with cell surface antibodies. These cells were further fixed and permeablized with FoxP3 Fix/Perm buffer kit from eBioscience according to the manufacturer's instructions and then stained with intracellular antibodies for further analysis by flow cytometry. For quantification, the absolute numbers of different cell types per gram of tumor were measured using CountBright Absolute Counting Beads (Life Technologies), which were added to each tumor specimen just before flow-cytometric analysis. For functional analysis, tumor-infiltrating T cells were restimulated with either 5×10^4 DCs loaded with B16 lysate or leukocyte activation mixture with Golgi-Plug (BD Biosciences) for 4 h at 37 °C before staining with cell surface and intracellular antibodies as described above. Data were acquired on BD LSR II cytometer and analyzed by FlowJo Software.

RNA Extraction from Tumors and Nanostring Analysis. Mice were challenged and treated as described above and humanely killed on day 14 to isolate tumors. Isolated tumors were dissociated in the presence of TRIzol reagent in GentleMACS M tubes by using the GentleMACS Dissociators. RNA was further extracted from dissociated tissue using RiboPure RNA purification kit by following the kit manufacturer's protocol. RNA purity was assessed on the ND-Nanodrop1000 spectrometer (Thermo Fisher Scientific). For Nanostring Assay, 100 ng of RNA was used to detect immune gene expression using nCounter Immunology panel. Counts of the reporter probes were tabulated for each sample by the nCounter Digital Analyzer and raw data output was imported into nSolver data analysis package (https://www.nanostring.com/products/analysis-software/nsolver)

to assess the quality of data and to perform the differential expression analysis. Volcano plot was made in GraphPad Prism 7.0 software.

Statistical Analysis. Data were analyzed with the GraphPad Prism 7.0 software program. Student's *t* test was used to assess differences between two groups for statistical significance. The Kaplan–Meier method was used to analyze survival data, and the log-rank (Mantel–Cox) test was used to assess differences in survival between different groups for statistical significance. Values of $P < 0.05$ were considered statistically significant.

ACKNOWLEDGMENTS. We thank Dr. Jeffrey V. Ravetch for providing FcγRIV KO mice, Dr. Andrew C. Chan for providing the anti-CD20 monoclonal antibody, Dr. David Tuveson for providing the mT5 cell line, Dr. Sreyashi Basu for helping with acquiring nanostring data, Nana-Ama A. Anang for providing technical assistance, and Dr. James Jeffrey Mancuso for reading and editing the manuscript. This work was supported by the Cancer Prevention Research Institute of Texas through Grant R1203 (to J.P.A.). J.V.'s laboratory is supported by funding from Canadian Institutes of Health Grant 86655.

1. Leach DR, Krummel MF, Allison JP (1996) Enhancement of antitumor immunity by CTLA-4 blockade. *Science* 271:1734–1736.
2. Hodi FS, et al. (2010) Improved survival with ipilimumab in patients with metastatic melanoma. *N Engl J Med* 363:711–723.
3. Sutmuller RP, et al. (2001) Synergism of cytotoxic T lymphocyte-associated antigen 4 blockade and depletion of $CD25^+$ regulatory T cells in antitumor therapy reveals alternative pathways for suppression of autoreactive cytotoxic T lymphocyte responses. *J Exp Med* 194:823–832.
4. Quezada SA, Peggs KS, Curran MA, Allison JP (2006) CTLA4 blockade and GM-CSF combination immunotherapy alters the intratumor balance of effector and regulatory T cells. *J Clin Invest* 116:1935–1945.
5. Simpson TR, et al. (2013) Fc-dependent depletion of tumor-infiltrating regulatory T cells co-defines the efficacy of anti-CTLA-4 therapy against melanoma. *J Exp Med* 210:1695–1710.
6. Curran MA, Montalvo W, Yagita H, Allison JP (2010) PD-1 and CTLA-4 combination blockade expands infiltrating T cells and reduces regulatory T and myeloid cells within B16 melanoma tumors. *Proc Natl Acad Sci USA* 107:4275–4280.
7. Waitz R, et al. (2012) Potent induction of tumor immunity by combining tumor cryoablation with anti-CTLA-4 therapy. *Cancer Res* 72:430–439.
8. Wolchok JD, et al. (2013) Nivolumab plus ipilimumab in advanced melanoma. *N Engl J Med* 369:122–133.
9. Fan X, Quezada SA, Sepulveda MA, Sharma P, Allison JP (2014) Engagement of the ICOS pathway markedly enhances efficacy of CTLA-4 blockade in cancer immunotherapy. *J Exp Med* 211:715–725.
10. Sharma P, Allison JP (2015) Immune checkpoint targeting in cancer therapy: Toward combination strategies with curative potential. *Cell* 161:205–214.
11. Krieg AM (2007) Development of TLR9 agonists for cancer therapy. *J Clin Invest* 117: 1184–1194.
12. Shirota Y, Shirota H, Klinman DM (2012) Intratumoral injection of CpG oligonucleotides induces the differentiation and reduces the immunosuppressive activity of myeloid-derived suppressor cells. *J Immunol* 188:1592–1599.
13. Singh M, Overwijk WW (2015) Intratumoral immunotherapy for melanoma. *Cancer Immunol Immunother* 64:911–921.
14. Dewan MZ, et al. (2012) Synergy of topical Toll-like receptor 7 agonist with radiation and low-dose cyclophosphamide in a mouse model of cutaneous breast cancer. *Clin Cancer Res* 18:6668–6678.
15. Dovedi SJ, et al. (2013) Systemic delivery of a TLR7 agonist in combination with radiation primes durable antitumor immune responses in mouse models of lymphoma. *Blood* 121:251–259.
16. Kauffman EC, Liu H, Schwartz MJ, Scherr DS (2012) Toll-like receptor 7 agonist therapy with imidazoquinoline enhances cancer cell death and increases lymphocytic infiltration and proinflammatory cytokine production in established tumors of a renal cell carcinoma mouse model. *J Oncol* 2012:103298.
17. Prins RM, et al. (2006) The TLR-7 agonist, imiquimod, enhances dendritic cell survival and promotes tumor antigen-specific T cell priming: Relation to central nervous system antitumor immunity. *J Immunol* 176:157–164.
18. Iribarren K, et al. (2015) Trial Watch: Immunostimulation with Toll-like receptor agonists in cancer therapy. *OncoImmunology* 5:e1088631.
19. Mauldin IS, et al. (2015) TLR2/6 agonists and interferon-gamma induce human melanoma cells to produce CXCL10. *Int J Cancer* 137:1386–1396.
20. Oldford SA, et al. (2010) A critical role for mast cells and mast cell-derived IL-6 in TLR2-mediated inhibition of tumor growth. *J Immunol* 185:7067–7076.
21. Schneider C, et al. (2004) Tumour suppression induced by the macrophage activating lipopeptide MALP-2 in an ultrasound guided pancreatic carcinoma mouse model. *Gut* 53:355–361.
22. Curtin JF, et al. (2009) HMGB1 mediates endogenous TLR2 activation and brain tumor regression. *PLoS Med* 6:e10.
23. Asprodites N, et al. (2008) Engagement of Toll-like receptor-2 on cytotoxic T-lymphocytes occurs in vivo and augments antitumor activity. *FASEB J* 22:3628–3637.
24. Geng D, et al. (2010) Amplifying TLR-MyD88 signals within tumor-specific T cells enhances antitumor activity to suboptimal levels of weakly immunogenic tumor antigens. *Cancer Res* 70:7442–7454.
25. Dasgupta G, et al. (2011) Engagement of TLR2 reverses the suppressor function of conjunctiva $CD4^+CD25^+$ regulatory T cells and promotes herpes simplex virus epitope-specific $CD4^+CD25^-$ effector T cell responses. *Invest Ophthalmol Vis Sci* 52:3321–3333.
26. Liu H, Komai-Koma M, Xu D, Liew FY (2006) Toll-like receptor 2 signaling modulates the functions of $CD4^+$ $CD25^+$ regulatory T cells. *Proc Natl Acad Sci USA* 103:7048–7053.
27. Cottalorda A, et al. (2006) TLR2 engagement on CD8 T cells lowers the threshold for optimal antigen-induced T cell activation. *Eur J Immunol* 36:1684–1693.
28. Caron G, et al. (2005) Direct stimulation of human T cells via TLR5 and TLR7/8: Flagellin and R-848 up-regulate proliferation and IFN-gamma production by memory $CD4^+$ T cells. *J Immunol* 175:1551–1557.
29. Komai-Koma M, Jones L, Ogg GS, Xu D, Liew FY (2004) TLR2 is expressed on activated T cells as a costimulatory receptor. *Proc Natl Acad Sci USA* 101:3029–3034.
30. Sharma N, Akhade AS, Qadri A (2013) Sphingosine-1-phosphate suppresses TLR-induced CXCL8 secretion from human T cells. *J Leukoc Biol* 93:521–528.
31. Lembo A, et al. (2003) Differential contribution of Toll-like receptors 4 and 2 to the cytokine response to *Salmonella enterica* serovar Typhimurium and *Staphylococcus aureus* in mice. *Infect Immun* 71:6058–6062.
32. Smith KD, et al. (2003) Toll-like receptor 5 recognizes a conserved site on flagellin required for protofilament formation and bacterial motility. *Nat Immunol* 4:1247–1253.
33. Vazquez-Torres A, et al. (2004) Toll-like receptor 4 dependence of innate and adaptive immunity to *Salmonella*: Importance of the Kupffer cell network. *J Immunol* 172: 6202–6208.
34. Adib-Conquy M, Scott-Algara D, Cavaillon JM, Souza-Fonseca-Guimaraes F (2014) TLR-mediated activation of NK cells and their role in bacterial/viral immune responses in mammals. *Immunol Cell Biol* 92:256–262.
35. Lu H, et al. (2011) TLR2 agonist PSK activates human NK cells and enhances the antitumor effect of HER2-targeted monoclonal antibody therapy. *Clin Cancer Res* 17: 6742–6753.
36. Chassin C, et al. (2009) TLR4- and TLR2-mediated B cell responses control the clearance of the bacterial pathogen, *Leptospira interrogans*. *J Immunol* 183:2669–2677.
37. Selby MJ, et al. (2013) Anti-CTLA-4 antibodies of IgG2a isotype enhance antitumor activity through reduction of intratumoral regulatory T cells. *Cancer Immunol Res* 1: 32–42.
38. Sharma A, et al. (2019) Anti-CTLA-4 immunotherapy does not deplete $FOXP3^+$ regulatory T cells (Tregs) in human cancers. *Clin Cancer Res* 25:1233–1238.
39. Romano E, et al. (2015) Ipilimumab-dependent cell-mediated cytotoxicity of regulatory T cells ex vivo by nonclassical monocytes in melanoma patients. *Proc Natl Acad Sci USA* 112:6140–6145.
40. Arce Vargas F, et al. (2018) Fc effector function contributes to the activity of human anti-CTLA-4 antibodies. *Cancer Cell* 33:649–663.e4.
41. Murray PJ, Wynn TA (2011) Protective and pathogenic functions of macrophage subsets. *Nat Rev Immunol* 11:723–737.
42. Pommier A, et al. (2013) Inflammatory monocytes are potent antitumor effectors controlled by regulatory $CD4^+$ T cells. *Proc Natl Acad Sci USA* 110:13085–13090.
43. Tiemessen MM, et al. (2007) $CD4^+CD25^+Foxp3^+$ regulatory T cells induce alternative activation of human monocytes/macrophages. *Proc Natl Acad Sci USA* 104:19446–19451.
44. Boj SF, et al. (2015) Organoid models of human and mouse ductal pancreatic cancer. *Cell* 160:324–338.
45. Furness AJ, Vargas FA, Peggs KS, Quezada SA (2014) Impact of tumour microenvironment and Fc receptors on the activity of immunomodulatory antibodies. *Trends Immunol* 35:290–298.
46. Bulliard Y, et al. (2013) Activating Fc γ receptors contribute to the antitumor activities of immunoregulatory receptor-targeting antibodies. *J Exp Med* 210:1685–1693.
47. Dahan R, et al. (2015) FcγRs modulate the anti-tumor activity of antibodies targeting the PD-1/PD-L1 Axis. *Cancer Cell* 28:285–295.
48. Peggs KS, Quezada SA, Chambers CA, Korman AJ, Allison JP (2009) Blockade of CTLA-4 on both effector and regulatory T cell compartments contributes to the antitumor activity of anti-CTLA-4 antibodies. *J Exp Med* 206:1717–1725.
49. Marabelle A, et al. (2013) Depleting tumor-specific Tregs at a single site eradicates disseminated tumors. *J Clin Invest* 123:2447–2463.
50. van Egmond M, Vidarsson G, Bakema JE (2015) Cross-talk between pathogen recognizing Toll-like receptors and immunoglobulin Fc receptors in immunity. *Immunol Rev* 268:311–327.
51. Tang M, et al. (2015) Toll-like receptor 2 activation promotes tumor dendritic cell dysfunction by regulating IL-6 and IL-10 receptor signaling. *Cell Rep* 13:2851–2864.
52. Ferron M, Vacher J (2005) Targeted expression of Cre recombinase in macrophages and osteoclasts in transgenic mice. *Genesis* 41:138–145.
53. van Elsas A, Hurwitz AA, Allison JP (1999) Combination immunotherapy of B16 melanoma using anti-cytotoxic T lymphocyte-associated antigen 4 (CTLA-4) and granulocyte/macrophage colony-stimulating factor (GM-CSF)-producing vaccines induces rejection of subcutaneous and metastatic tumors accompanied by autoimmune depigmentation. *J Exp Med* 190:355–366.